# Dynamic *p*-Cycle Protection in Spectrum-Sliced Elastic Optical Networks

Fan Ji, Xiaoliang Chen, Wei Lu, Joel J. P. C. Rodrigues, and Zuqing Zhu, *Senior Member, IEEE*

***Abstract*—We investigate dynamic pre-configured-cycle (*p*-cycle) protection design for spectrum-sliced elastic optical networks (EONs). Several novel algorithms are proposed to use the spectrum planning of working and backup resources. We first combine the protected working capacity envelope (PWCE) *p*-cycle design with spectrum planning, and design an algorithm that can achieve dynamic *p*-cycle design in EONs. Then, to resolve the coverage issue of the PWCE-*p*-cycles, we consider dynamic *p*-cycle design with Hamiltonian cycles and propose to use topology partition for reducing the lengths of backup paths. Simulation results show that our proposed algorithms achieve lower blocking probability than the shared path-protection (SPP) algorithm, while the average length of backup paths per request can be controlled well. To the best of our knowledge, this is the first attempt to address dynamic *p*-cycle protection design with spectrum planning for EONs.**

***Index Terms*—Elastic optical networks (EONs), Hamiltonian cycle, preconfigured cycle (*p*-cycle), topology partition.**

## I. Introduction

NOWADAYS, the spectrum-sliced elastic optical networking based on the optical orthogonal frequency-division multiplexing (O-OFDM) technology [1] has attracted intensive research interests as it can improve the spectral efficiency of the optical layer significantly with flexible bandwidth allocation [2]. Unlike the wavelength-division multiplexing (WDM) networks that operate on discrete wavelength channels with a bandwidth of 50 or 100 GHz, the O-OFDM networks groom the capacities of a few narrow-band ($\sim$ 12.5 GHz) subcarrier channels (frequency slots) that are spectrally contiguous and achieve high-speed data transmission over them. Hence, by adjusting the number of assigned frequency slots (FS') to each lightpath, O-OFDM networks can allocate optical spectrum with a finer granularity and agile bandwidth management for different network applications can be achieved [3]. To this end, people refer the optical networks based on the O-OFDM technology as elastic optical networks (EONs) [4]–[6].

Previously, researchers have investigated the routing and spectrum assignment (RSA) of lightpaths intensively for realizing efficient service planning and provisioning in EONs [4]–[9]. However, most of these studies did not consider how to setup lightpath connections with protection or restorability. It is known that in optical networks, the amount of service disruption and data loss caused by a network-related outage can be huge [10], because a single optical fiber can carry over 20 Tb/s transmission capacity [11]. Meanwhile, natural disasters and other factors can trigger unpredictable failures of network elements and make network survivability a serious issue [10]. In EONs, a link failure may lead to more severe service disruption due to the higher data-rate provided by the supper-channels. Therefore, it is not only important but also necessary to study the protection schemes for EONs, and the network operators need to implement them to ensure certain service availability for the lightpath connections.

In [12], under the assumption that the bandwidth allocation of the protect path could be less than that of the working path, Sone *et al.* proposed a bandwidth squeezed restoration scheme for dedicated path-protection (DPP) in EONs. Based on $K$ shortest-path routing and first-fit spectrum assignment, a shared path-protection (SPP) scheme was developed for EONs in [13] to enhance the protection efficiency. In order to fully utilize EON's spectral segments for path-protection, Castro *et al.* proposed a single-path provisioning and multi-path recovery scheme in [14]. They considered both the DPP and SPP schemes, and provided mixed integer linear programming (MILP) formulations to optimize the protection designs. The problem of static RSA for EONs with DPP was investigated in [15], where the authors formulated an integer linear programming (ILP) model and proposed an adaptive frequency assignment with DPP heuristic to obtain the near-optimal solutions. In [16], Eira *et al.* studied the problem of static RSA for translucent EONs with SPP, and designed both an ILP model and a heuristic to solve it. A DPP scheme for adaptive combinational quality-of-transmission (QoT) degradation restoration in EONs was experimentally demonstrated in [17]. The authors of [18] proposed an SPP scheme for EONs, which was called elastic separate-protection-at-connection and could realize spectrum sharing by using first-fit to assign working traffic and last-fit to assign backup traffic.

Manuscript received September 20, 2013; revised November 24, 2013 and January 9, 2014; accepted January 9, 2014. Date of publication January 13, 2014; date of current version February 3, 2014. This work was supported in part by the Program for New Century Excellent Talents in University (NCET) under Project NCET-11-0884, the National Natural Science Foundation of China under Project 61371117, the Fundamental Research Funds for the Central Universities (WK2100060010), the Strategic Priority Research Program of the Chinese Academy of Sciences (XDA06010302), the Instituto de Telecommunicações, Next Generation Networks and Applications Group (NetGNA), Portugal, and National Funding from the FCT—Fundação para a Ciência e Tecnologia through the Pest-OE/EEI/LA0008/2013.

F. Ji, X. Chen, W. Lu, and Z. Zhu are with the School of Information Science and Technology, University of Science and Technology of China, Hefei, Anhui 230027, China (e-mail: angelajf@mail.ustc.edu.cn; arabus@mail.ustc.edu.cn; luwei11@mail.ustc.edu.cn; zqzhu@ieee.org).

J. J. P. C. Rodrigues is with the Instituto de Telecommunicações, University of Beira Interior, 6201-001 Portugal (e-mail: joeljr@ieee.org).

Color versions of one or more of the figures in this paper are available online at http://ieeexplore.ieee.org.

Digital Object Identifier 10.1109/JLT.2014.2300337

Generally, the aforementioned path-protection schemes allocate two disjoint lightpaths to each connection as its working and backup paths. Even though these schemes are straightforward to implement, they may suffer from relatively long restoration time, as the backup resources are only reserved but not pre-configured and when a link failure happens, we need to re-configure all the nodes along the working and backup paths for restoration [10]. More importantly, setting up and tearing down working and backup paths frequently in dynamic network provisioning can result in spectrum fragmentation and degrade the EON's blocking probability [19]. Therefore, it is desired to explore other protection schemes for EONs.

The concept of pre-configured-cycles (*p*-cycles) was introduced in [20] for link-protection. Specifically, a *p*-cycle is pre-configured to protect a working link, and when the link fails, the *p*-cycle is activated for restoration by reconfiguring its two end-nodes. Therefore, the restoration only involves the two nodes that are directly connected to the broken link, resulting in a relatively short recovery time. Another unique advantage of *p*-cycles is that they can protect not only the links that are on-cycle but also those that straddle them. More specifically, one unit bandwidth on a *p*-cycle can protect one unit on each on-cycle link that is in its opposite direction, and can also protect two units on each pair of its straddling links (one unit in each direction). Due to these advantages, network resilience with *p*-cycles has been studied intensively in WDM networks [20]–[25]. Moreover, the protected working capacity envelope (PWCE) [26] technique can be used together with *p*-cycles for protection design. Specifically, for a given network, PWCE sets up a set of *p*-cycles that can protect all the links and reserves certain spectrum resources on the *p*-cycles to establish a backup layer in the spectrum domain. Therefore, when a lightpath request is provisioned in the network, all the links in its working path are protected by the resources in the backup layer automatically. By doing so, PWCE saves the efforts on computing protection structure for each individual request, and reduces the complexity of network operation and management, especially for dynamic network environments where the requests can arrive and leave on the fly.

Even though the protection schemes based on *p*-cycle and PWCE had exhibited the aforementioned benefits in WDM networks, their implementations in EONs are still under-explored. In this paper, we investigate dynamic *p*-cycle protection design for EONs with connections being set up and torn down dynamically, and propose several algorithms. First, by combining PWCE-*p*-cycle design with spectrum planning, we propose an algorithm that can achieve dynamic *p*-cycle design in EONs. Then, in order to resolve the coverage issue of the PWCE-*p*-cycles, we consider dynamic *p*-cycle design with Hamiltonian cycles and propose to use topology partition for reducing the lengths of backup paths. The simulation results show that our proposed algorithms can achieve lower blocking probability than the SPP algorithm.

The rest of the paper is organized as follows. Section II describes the working principle of *p*-cycle protection design in EONs. In Sections III and IV, we discuss the *p*-cycle protection designs with PWCE and Hamiltonian cycles. The performance of the proposed algorithms is evaluated in Section V. Finally, Section VI summarizes the paper.

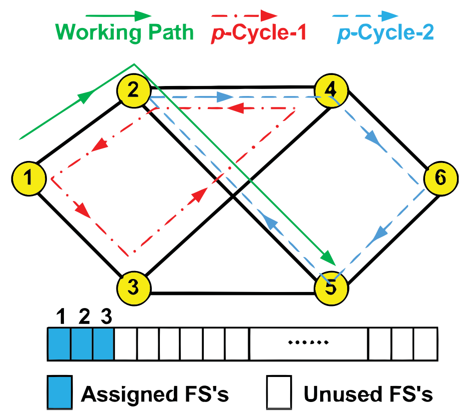


Fig. 1. Same-spectrum *p*-cycle protection in EONs.

## II. *p*-CYCLE PROTECTION IN EONS

In this section, we explain the working principles of *p*-cycle protection in EONs. In a given EON topology denoted as $G(V,E)$ where $V$ and $E$ represent the node set and the set of directed fiber links, we have a request as $LR(s,d,n)$ where $s$ and $d$ are the source and destination nodes $(s,d \in V)$ and $n$ is the requested bandwidth in terms of the number of contiguous frequency slots (FS'). We assume all the requests are carried by lightpaths all-optically without any spectrum converters or optical-electrical-optical (O/E/O) converters in the intermediate node(s), and hence the block of contiguous FS' used for a request should be identical on all the fiber links in its routing path $\mathcal{R}_{s,d}$, i.e., satisfying the spectrum continuity and contiguous constraints [5]. Then, to protect the FS' allocated on each link in the working path $\mathcal{R}_{s,d}$, we configure *p*-cycle(s) and allocate necessary spectrum resources. Similarly, in order to minimize spectrum converters and O/E/O converters in the EONs, the backup resources allocated to the *p*-cycle(s) should use the same FS' as those on the working path. We call this scheme as "same-spectrum" *p*-cycle protection. Note that this "same-spectrum" policy does not limit the generality of our work. In the EONs that do not comply to it, we can simply place two spectrum converters at the two ends of the protected link, while the *p*-cycle construction is still the same. If we assume that each link $e \in E$ can accommodate $F$ FS', the indices of the FS' on each link are in the range of $[1,F]$. For a request, the starting and ending indices of the allocated FS' are $f_s$ and $f_e$, respectively, and we have

$$f_e - f_s = n - 1, \quad f_e, f_s \in [1,F]. \tag{1}$$

Fig. 1 shows an intuitive example of the same-spectrum *p*-cycle protection in EONs. The working path of $LR(1,5,3)$ consists of two links, 1→2 and 2→5, which are protected by *p*-cycle 1→3→4→2→1 and *p*-cycle 2→4→6→5→2, respectively. The working path and two *p*-cycles use the same FS', as $f_s = 1$ and $f_e = 3$.

The major advantage of $p$-cycle protection lies in the relatively short restoration time, while it may have drawbacks as low protection efficiency since a $p$-cycle is configured for each link in the working path. Moreover, the fine bandwidth allocation granularity in EONs may cause spectrum fragmentation [19] and degrade the blocking performance. To address these issues, we discuss $p$-cycle protection design algorithms that incorporate spectrum planning to regulate the spectra of working and backup resources in the following sections.

## III. $p$-Cycle Protection Design With PWCE Cycles

In this section, we introduce a $p$-cycle protection design algorithm that adopts the protected working capacity envelop (PWCE) [26] and spectrum planning (SP). More specifically, we first obtain a set of $p$-cycles that can protect all links in the topology $G(V, E)$, and then partition the total spectrum resources in the EON logically into the working, backup and hybrid FS-layers under the PWCE concept. The working FS-layer contains the FS' that can be allocated to the working paths of the requests, the backup FS-layer is for the FS' that are reserved to configure $p$-cycles, and the hybrid FS-layer contains the rest of the FS', which can be used for either working paths or $p$-cycles. Spectrum planning establishes static backup resources in the spectrum domain and achieves efficient protection, since the frequent setting up and tearing down of $p$-cycles can be minimized and hence the spectrum fragmentation is reduced in a dynamic network environment.

### A. PWCE-p-Cycle Design

With the physical topology $G(V, E)$, we calculate a large set of cycles and store them in $\mathbb{C}$. Note that for practicalness, the "large set of cycles" here only includes a subset of all the cycles in the topology, as the number of cycles in a topology generally increases exponentially with the number of nodes. For example, with the 14-node NSFNET topology in Fig. 2(a), we calculate 518 shortest cycles with the algorithm in [25] and store them in $\mathbb{C}$. In order to select the PWCE-$p$-cycles from $\mathbb{C}$, we formulate an ILP model whose objective is to minimize the total number of links in the selected cycles. The rationale behind this objective is that with the minimum total number of links in the PWCE-$p$-cycles, we achieve the highest protection efficiency.

*Notations:*

1) $\mathbb{C}$: The large set of cycles in $G(V, E)$.
2) $\mathcal{C}_k$: The $k$-th cycle in $\mathbb{C}$.
3) $|\mathcal{C}_k|$: The number of links in the $k$-th cycle $\mathcal{C}_k$.
4) $y_{e,k}$: The flag that equals 1, if a link $e$ can be protected by the cycle $\mathcal{C}_k$, and 0 otherwise.
5) $w_{e,k}$: The flag that equals 1, if a link $e$ is on the cycle $\mathcal{C}_k$, and 0 otherwise.
6) $\gamma$: The preset threshold that the number of links in a selected cycle cannot exceed.

*Variables:*

1) $x_k$: Boolean variable that equals 1 if $\mathcal{C}_k$ is selected, and 0 otherwise.
2) $m_e$: Boolean variable that equals 0 or 1.

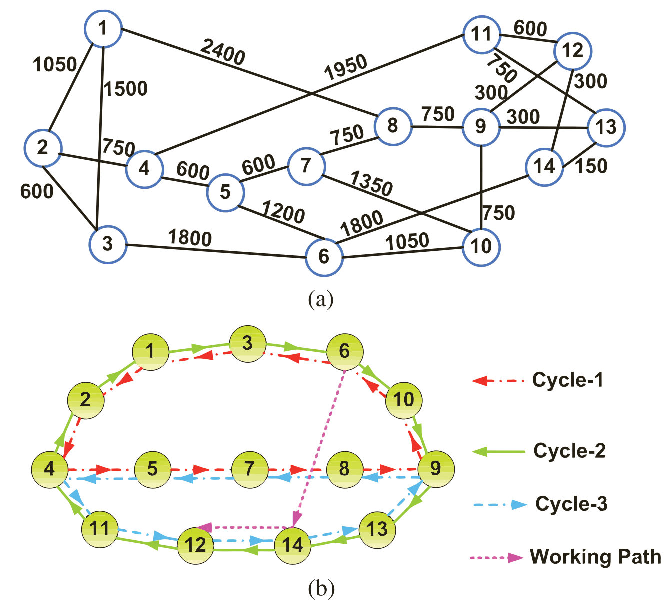


Fig. 2. Example of PWCE-$p$-cycle configuration. (a) NSFNET topology (fiber lengths in kilometers). (b) Configurations of PWCE-$p$-cycles.

*Objective:*

$$\text{Minimize} \qquad z = \sum_e m_e. \tag{2}$$

*Constraints:*

$$\sum_k x_k \cdot y_{e,k} > 0, \quad \forall e \in E. \tag{3}$$

Equation (3) ensures that all the links in $G(V, E)$ are protected by the selected cycles.

$$x_k \cdot |\mathcal{C}_k| \leq \gamma, \quad \forall k. \tag{4}$$

Equation (4) ensures that the number of links in each selected cycle does not exceed the preset threshold $\gamma$.

$$m_e \geq \frac{1}{|E|} \cdot \sum_k x_k \cdot w_{e,k}, \quad \forall e \in E \tag{5}$$

where $|E|$ returns the total number of links in $G(V, E)$. Equation (5) ensures that each link only gets counted once towards the total number of links in the selected cycles.

For $p$-cycle protection design with PWCE cycles in EONs, we solve this ILP once in the network initialization and obtain the cycles to form the PWCE-$p$-cycles. Since there is no need to solve it again afterwards, this ILP will not cause intolerable computational complexity or affect the speed of restoration during network operation.

### B. Spectrum Planning

Spectrum planning logically partitions the total spectrum resources in the EON into the working, backup and hybrid FS-layers. Note that certain requests can require more than one PWCE-$p$-cycles for protection. For such a request, because of the same-spectrum policy, its $p$-cycles have to use the same block of FS'. However, due to the intrinsic limitation of PWCE-*p*-cycles, some of the *p*-cycles may not be able to use the same block of FS'. Therefore, we have to allocate the hybrid FS-layer, and the specific explanation is given by the following example.

With the NSFNET topology in Fig. 2(a) where each line corresponds to two directed links, the ILP obtains the three PWCE-*p*-cycles in Fig. 2(b) for $\gamma = 11$. Apparently, the three *p*-cycles, i.e., *Cycles* 1-3, have to use non-overlapped FS' for their backup FS-layers. Otherwise, there will be non-allocatable FS' that cannot be used for either working or backup. For instance, let us consider the situation where the backup FS-layers on *Cycles* 1 and 2 share the same FS block $[f_s, f_e]$. Then, due to the same-spectrum policy, FS' $[f_s, f_e]$ on *Cycle* 1 protect working FS' $[f_s, f_e]$ on link 6→10. However, link 6→10 is on *Cycle* 2 and FS' $[f_s, f_e]$ on it have already been allocated to the backup FS-layer. Therefore, the FS' $[f_s, f_e]$ on link 6→10 cannot be used for either working or backup and become a block of non-allocatable FS'.

Since *Cycles* 1-3 have to use different and non-overlapped FS' for their backup FS-layers, we will face an issue that makes the allocation of the hybrid FS-layers necessary. Still in Fig. 2(b), let us consider the working path 6→14→12, and it can be seen that link 6→14 can be protected by *Cycle* 2, but link 14→12 can only be protected by *Cycle* 3. Since there is no spectrum overlapping between the backup FS-layers of *Cycles* 2 and 3, we cannot find a feasible block of FS' in the working FS-layers to serve the working path 6→14→12, based on the same-spectrum policy. Therefore, we have to assign the hybrid FS-layer on each link to solve this issue.

Note that for different links, the partitions of the working, backup and hybrid FS-layers can be different. The actual spectrum planning of the working, backup and hybrid FS-layers can be based on the traffic model, and when the traffic prediction between each node pair is roughly known, we can assign the blocks of FS' in an empirical way. If we need to protect all the working paths against single-link failures, the sizes of the working FS-layer and its corresponding backup FS-layer should be equal. *Algorithm* 1 shows the generic procedure of the spectrum planning. Basically, the spectrum planning can be modeled as a graph coloring problem and solved with an auxiliary graph. For instance, with the PWCE-*p*-cycles in Fig. 2(b), *Algorithm* 1 obtains the auxiliary graph as shown in Fig. 3(a) and finds $\Upsilon = 3$, i.e., we need at least three colors to color the nodes in $G^a(V^a, E^a)$ and have to divide the whole FS' on links into four FS-blocks. Fig. 3(b) shows the actual spectrum planning for *Cycles* 1-3 and the straddling link 6→14, which is on none of the PWCE-*p*-cycles.

**Algorithm 1:** Spectrum Planning for PWCE-*p*-cycle

calculate a large set of cycles in $G(V, E)$;
store the cycles in $\mathbb{C}$;
solve ILP in Subsection III.A to obtain the PWCE-*p*-cycles from $\mathbb{C}$;
$i = 0$;
**for** *all the PWCE-p-cycles* **do**
  $i = i + 1$;
  denote the PWCE-*p*-cycle as $\mathcal{C}_i^P$;
  insert a node $v_i^a$ in the auxiliary graph $G^a(V^a, E^a)$;
  **for** $j = 1 \cdots i$ **do**
    **if** $\mathcal{C}_i^P$ *and* $\mathcal{C}_j^P$ *cannot have the same FS assignment for their backup FS-layers* **then**
      connect $v_i^a$ and $v_j^a$ in $G^a(V^a, E^a)$;
    **end**
  **end**
**end**
solve the graph coloring problem in $G^a(V^a, E^a)$;
denote the minimum number of colors as $\Upsilon$;
divide the whole FS' into $\Upsilon$+1 equal blocks;
assign FS blocks on the PWCE-*p*-cycles as backup FS-layers according to the solution of coloring problem;
assign corresponding FS blocks on the links that are protected by the PWCE-*p*-cycles as working FS-layers;
assign the rest FS blocks on all links $e \in E$ as hybrid FS-layers;

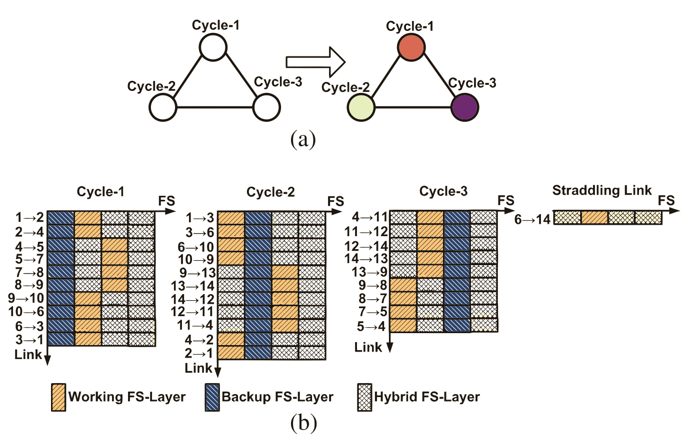


Fig. 3. Example of spectrum planning for PWCE-*p*-cycles. (a) The coloring map. (b) Spectrum planning.

## C. Protection-Enabled RSA

For each request, we first try to serve it in the working FS-layer with $K$ shortest-path routing and first-fit spectrum assignment (KSP-FF-RSA). If the request can be served with the spectrum resources in the working FS-layer, the corresponding backup resources will be allocated automatically in the PWCE-*p*-cycles. Otherwise, we try to serve the request in the hybrid FS-layer, which includes establishing the working path with KSP-FF-RSA and then assembling *p*-cycles to protect all the links in the working path under the same-spectrum constraint.

We call this algorithm as PWCE based *p*-cycle design with spectrum planning (PWCE-*p*-cycle-SP), and *Algorithm* 2 shows the detailed procedure. *Line* 1 is for the network initialization with spectrum planning. *Lines* 3-7 explain how to achieve protection-enabled RSA in the working and backup FS-layers

**Algorithm 2:** PWCE-*p*-cycle-SP Algorithm

```
1  run Algorithm 1 to get spectrum planning;
2  for each incoming request LR(s, d, n) do
3      calculate K shortest paths from s to d;
4      for each candidate routing path R_{s,d} do
5          if enough resources exist in the path's working
           FS-layer then
6              provision LR;
7              break;
8          else
9              try KSP-FF-RSA for working path RSA of
               LR in the hybrid FS-layer;
10             if the working path RSA succeeds then
11                 for all links in the working path do
12                     try to protect it with existing p-cycles
                       in the hybrid FS-layer;
13                     if shared protection is failed then
14                         try to assemble a new p-cycle in
                           the hybrid FS-layer with the
                           highest protection efficiency;
15                     end
16                 end
17                 if the working and backup resources of
                   LR are reserved then
18                     provision LR;
19                     break;
20                 end
21             end
22         end
23     end
24     if the working and backup resources of LR cannot
       be reserved then
25         mark LR as blocked;
26     end
27 end
```

based on PWCE-*p*-cycles. Then, *Lines* 9-22 show the procedure to perform protection-enabled RSA in the hybrid FS-layer, in which the *p*-cycles are assembled on demand. Note that we allow multiple working paths to share the same *p*-cycle as long as they are link-disjoint, as shown in *Line* 12. *Lines* 13-15 indicate that when a new *p*-cycle has to be assembled in the hybrid FS-layer, we select the one that has the highest protection efficiency. Here, if a *p*-cycle $\mathcal{C}_k$ can protect $M$ links simultaneously in the working path $\mathcal{R}_{s,d}$, we define the protection efficiency of $\mathcal{C}_k$ for $\mathcal{R}_{s,d}$ as

$$\eta(\mathcal{R}_{s,d}, \mathcal{C}_k) = \frac{M}{|\mathcal{C}_k|}, \quad (6)$$

where $|\mathcal{C}_k|$ returns the number of links in $\mathcal{C}_k$.

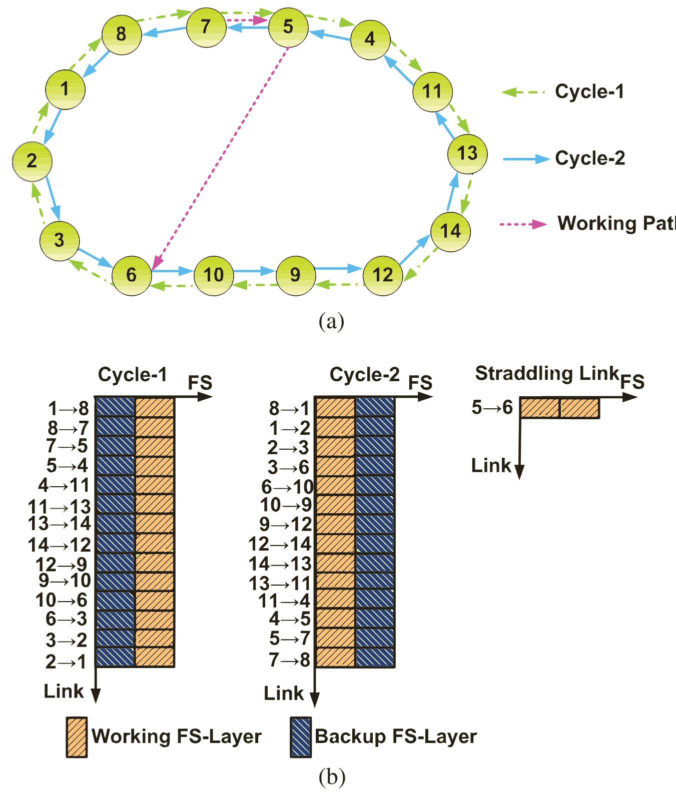


Fig. 4. Spectrum planning in Ham-*p*-cycle-SP algorithm. (a) Configurations of Hamiltonian-*p*-cycles. (b) Spectrum planning.

## IV. *p*-Cycle Protection Design With Hamiltonian Cycles

It can be seen that for PWCE-*p*-cycle-SP, the protection-enabled RSA in the hybrid FS-layer increases computational complexity and causes spectrum fragmentation, since the *p*-cycles still need to be assembled on demand. It is known that in a mesh topology with proper connectivity, we can obtain Hamiltonian cycles that traverse all nodes in the topology only once [22]. For instance, the Hamiltonian cycles in Fig. 4(a) for the NSFNET topology in Fig. 2(a). Hence, all the links in the topology can be protected by the two Hamiltonian *p*-cycles that have the same connections but are in the opposite directions, since any of the links is either an on-cycle or a straddling link of them. To this end, the coverage issue in Fig. 2(b) for PWCE-*p*-cycles can be resolved by replacing the PWCE cycles with Hamiltonian cycles. Consequently, the hybrid FS-layer can be removed from the spectrum planning.

### A. *Hamiltonian-p-Cycle Design*

With the physical topology $G(V, E)$, we first find the Hamiltonian cycles with a stochastic optimization algorithm, for example, the ant colony optimization (ACO). For instance, with the NSFNET topology in Fig. 2(a), we can obtain two directed Hamiltonian cycles as *Cycles* 1-2 in Fig. 4(a). The characteristic of Hamiltonian cycle guarantees that we only have two nodes in the auxiliary graph for the coloring problem. Hence, the

**Algorithm 3:** Ham-*p*-cycle-SP Algorithm

1 calculate Hamiltonian cycles;
2 partition link spectrum into working and backup FS-layers based on the two Hamiltonian-*p*-cycles;
3 **for** *each incoming request* $LR(s, d, n)$ **do**
4   calculate $K$ shortest path candidates from $s$ to $d$;
5   **for** *each path candidate* $\mathcal{R}_{s,d}$ **do**
6     **if** *enough resources exist in the path's working FS-layer* **then**
7       provision $LR$;
8       **break**;
9     **end**
10   **end**
11   **if** *the working and backup resources of* $LR$ *cannot be reserved* **then**
12     mark $LR$ as blocked;
13   **end**
14 **end**

spectrum resources can be divided equally into two FS blocks and the spectrum planning of the working and backup FS-layers is straightforward, since there is no need to allocate the hybrid FS-layer any more. Fig. 4(b) shows the results of the spectrum planning, for the *p*-cycles and the straddling link 5→6. For this Hamiltonian cycle based *p*-cycle design with spectrum planning (Ham-*p*-cycle-SP), the premise is the existence of a Hamiltonian cycle in the network topology. Thanks to the relatively high connectivity of core networks, Hamiltonian cycles can usually be found.

### B. Ham-p-Cycle-SP Algorithm

In Ham-*p*-cycle-SP, the spectrum planning logically divides the spectrum resources into the working and backup FS-layers. The working FS-layer contains the FS' that can be allocated to the working paths of the requests, while the FS' in the backup layer are reserved to configure the Hamiltonian-*p*-cycles. Note that the partitions of the working and backup FS-layers are only for the on-cycle links, while the whole spectrum resources on the straddling links can be used for working paths. For instance, for the working path 7→5→6 in Fig. 4(a), *Link* 7→5 is an on-cycle link and we can only use the FS' in the working FS-layer for the working path, while *Link* 5→6 is a straddling link and all its spectrum are allocated to the working FS-layer, as in Fig. 4(b). For a request, if its working path can be served in the working FS-layer successfully, it is protected against single-link failures by the Hamiltonian-*p*-cycles automatically.

*Algorithm* 3 shows the details of Ham-*p*-cycle-SP. It can be seen that because the hybrid FS-layer is removed, *Algorithm* 3 is much simpler than *Algorithm* 2. *Lines* 4-10 describe the protection-enabled RSA based on Hamiltonian-*p*-cycles. Note that in *Line* 5, we check the candidate routing paths of $LR$ in ascending order of their numbers of hops.

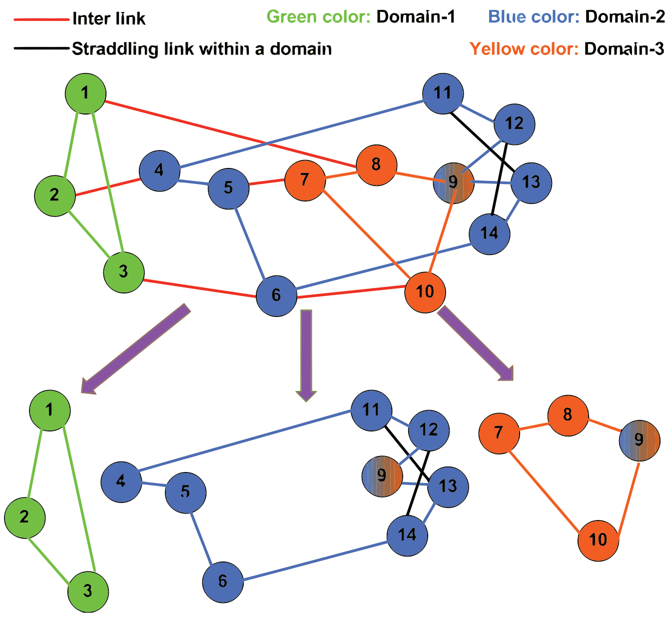


Fig. 5. Topology partition in NSFNET topology.

### C. Hamiltonian-p-Cycle Design With Topology Partition

One major issue with Ham-*p*-cycle-SP is that it can provide a very long protection path. For example, in Fig. 4(a), if Link 7→5 fails, the Hamiltonian-*p*-cycle needs to use the backup path from *Node* 7 to *Node* 5 on *Cycle* 2 to recover the service. However, the backup path consists of 13 hops and therefore can cause excessive delay as well as intolerable physical impairments. Another issue is that Hamiltonian cycle may not always exist in an arbitrary network topology.

In order to address these issues, we discuss Hamiltonian-*p*-cycle design with topology partition in this section. Fig. 5 shows an example of topology partition in the NSFNET topology. We partition the topology into three domains whose nodes are in different colors. Note that *Node* 9 belongs to two domains simultaneously, i.e., *Domains* 2 and 3. Inside each domain, the on-cycle links (*e.g.*, *Link* 1→2) are colored with the same color as the nodes, while the straddling links (*e.g.*, *Link* 11→13) are in black. In addition to these "intra-links" that are within a domain, there are also inter-domain links that connect the domains together, e.g., *Link* 1→8, and we define them as "inter-links" and mark them as red in Fig. 5.

The topology partition is equivalent to the problem of finding a few cycles that together can cover all the nodes in the topology. Then, the nodes on each cycle and the corresponding intra-links compose a domain and the cycle is the domain's Hamiltonian cycle. We formulate the ILP model below to solve the problem of topology partition. The ILP is also based on a large set of pre-calculated cycles in the topology, which is the same as that in the ILP model in Section III-A.

*Notations:*

1) $\mathbb{C}$: The large set of cycles in $G(V, E)$.
2) $\mathcal{C}_k$: The $k$th cycle in $\mathbb{C}$.
3) $|\mathcal{C}_k|$: The number of links in the $k$th cycle $\mathcal{C}_k$.
4) $|E|$: The number of links in the topology.

5) $y_{e,k}$: The flag that equals 1 if $\mathcal{C}_k$ can protect link $e \in E$, and 0 otherwise.
6) $\psi_{v,k}$: The flag that equals 1 if $\mathcal{C}_k$ traverses node $v \in V$, and 0 otherwise.
7) $\gamma$: The preset threshold that the number of links in a selected cycle cannot exceed.

*Variables:*

1) $x_k$: Boolean variable that equals 1 if $\mathcal{C}_k$ is selected, and 0 otherwise.

*Objective:*

Basically, we want to minimize the total number of inter-links, as the working resources on them cannot be protected by the intra-domain *p*-cycles. Hence, we design the objective as

$$\text{Minimize} \quad z = |E| - \sum_k \sum_{e \in E} x_k \cdot y_{e,k}. \tag{7}$$

*Constraints:*

$$\sum_k \psi_{v,k} \cdot x_k \geq 1, \quad \forall v \in V. \tag{8}$$

Equation (8) ensures that each node $v \in V$ belongs to at least one domain.

$$x_k \cdot |\mathcal{C}_k| \leq \gamma, \quad \forall k. \tag{9}$$

Equation (9) ensures that the number of links in each selected cycle does not exceed the preset threshold $\gamma$.

$$\sum_k \sum_{e \in E} x_k \cdot y_{e,k} \leq 1. \tag{10}$$

Equation (10) ensures that the selected cycles do not share common intra-links. Similar to the case in Subsection III.A, since we only need to solve this ILP once for topology partition in the network initialization, it will not affect the speed of restoration during network operation.

With the domains designed, we apply Ham-*p*-cycle-SP to each domain and protect the working resources on the intra-links. While for the inter-links, we construct two inter-domain *p*-cycles to protect them. More specifically, we first build a *p*-cycle that traverses all the end-nodes of the inter-links, and then construct the other one with the same connections but in the opposite direction. Note that in this case, not all the nodes in the *p*-cycles can be pre-configured, since the inter-domain and intra-domain *p*-cycles can share the same FS' on link(s) for high protection efficiency. Basically, when an inter-domain *p*-cycle shares link(s) with an intra-domain one, the "exit-node(s)" (*i.e.*, the node(s) where the link sharing ends) of the shared link(s) cannot be pre-configured. When a link failure happens, the network first determines whether it is on an inter-link. If yes, then the network instructs the "exit-node(s)" to activate the corresponding inter-domain *p*-cycle. Otherwise, the related intra-domain *p*-cycle is activated. As some of the nodes cannot be pre-configured, the restoration time can be prolonged, but the benefit is that we obtain high protection efficiency from the spectrum sharing among the inter- and intra-domain *p*-cycles. Previous studies have also investigated this type of modification on *p*-cycle to improve the protection efficiency [27], [28]. In the rest of the paper, we refer to this modified Ham-*p*-cycle-SP algorithm as partitioned Ham-*p*-cycle-SP (P-Ham-*p*-cycle-SP).

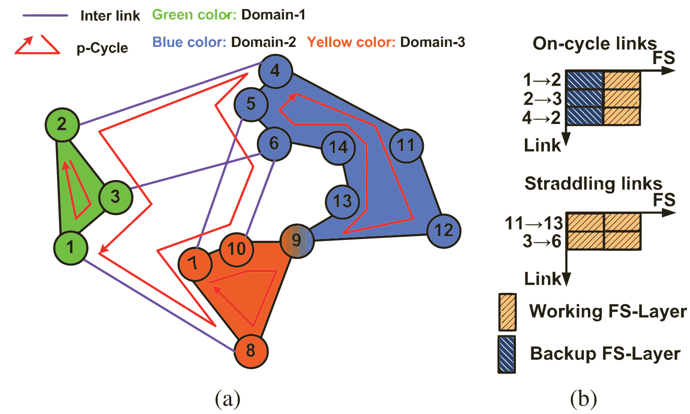


Fig. 6. Hamiltonian *p*-cycle design and spectrum planning in NSFNET with topology partition. (a) *p*-Cycle design. (b) Spectrum planning.

Fig. 6 shows an example of Hamiltonian *p*-cycle design and spectrum planning for P-Ham-*p*-cycle-SP. With the topology partition in Fig. 5, we construct the Hamiltonian *p*-cycles and $\mathcal{C}^+_{\text{inter}}$ as shown in Fig. 6(a). Note that we only include half of the *p*-cycles here, as the rest of the *p*-cycles have the same connection but are in the opposite directions. Since the inter-domain *p*-cycle 2→3→1→8→7→10→6→5→4→2 and the intra-domain *p*-cycle 2→3→1→2 share the same links 2→3 and 3→1, *Node* 1 becomes the "exit-node" of the shared links. Then, if the intra-link 3→2 fails, the network instructs *Node* 1 to activate the protection segment 3→1→2. On the other hand, if the inter-link 2→4 fails, *Node* 1 activates the protection segment 2→3→1→8→7→10→6→5→4. The spectrum planning results of the on-cycle links, such as *Links* 1→2, 2→3 and 4→2, and the straddling links, such as *Links* 11→13 and 3→6 are shown in Fig. 6(b).

*Algorithm* 4 shows the details of how to construct *p*-cycles and conduct spectrum planning in P-Ham-*p*-cycle-SP. *Lines* 1-3 are for initialization. An inter-domain *p*-cycle for inter-links, $\mathcal{C}^+_{\text{inter}}$, is constructed in *Line* 4, which traverses all the end-nodes of the inter-links. Then, a pair of inter-domain *p*-cycles in the opposite directions, $\mathcal{C}^+_{\text{inter}}$ and $\mathcal{C}^-_{\text{inter}}$, can protect all the inter-links, since each inter-link is either an on-cycle link or a straddling link of them. *Lines* 5-6 are for the spectrum planning on $\mathcal{C}^+_{\text{inter}}$. The spectrum planning for the intra-domain Hamiltonian *p*-cycles is conducted with *Lines* 7-20. Basically, for each domain, if any of the two Hamiltonian *p*-cycles shares link(s) with $\mathcal{C}^+_{\text{inter}}$, we make sure that the FS-layers of it are assigned exactly the same as those on $\mathcal{C}^+_{\text{inter}}$. Hence, the working path that traverses multiple domains can be protected efficiently. Otherwise, if there are no shared links, we just select either of the intra-domain Hamiltonian *p*-cycles and implement the FS-layer assignment of $\mathcal{C}^+_{\text{inter}}$ on it, as shown in *Lines* 16-19. When $\mathcal{C}^+_{\text{inter}}$ and the related intra-domain Hamiltonian *p*-cycles are taken care of, we build the *p*-cycle $\mathcal{C}^-_{\text{inter}}$ in the opposite direction, and perform the spectrum planning procedure in the opposite way, as shown in *Lines* 21-24. In *Line* 25, all FS' on the straddling links in $G(V, E)$ are assigned as the working FS-layer.

**Algorithm 4:** *p*-cycle Design and Spectrum Planning for P-Ham-*p*-cycle-SP

```
1  calculate a large set of cycles in G(V, E);
2  store the cycles in ℂ;
3  solve ILP in Subsection IV.C to partition the topology;
4  construct p-cycle C+_inter that traverses all the end-nodes
   of the inter-links;
5  assign FS' [1, ⌈F/2⌉] on C+_inter as working FS-layer;
6  assign FS' [⌈F/2⌉ + 1, F] on C+_inter as backup FS-layer;
7  for each domain in the topology do
8      flag = FALSE;
9      for the two intra-domain Hamiltonian p-cycles do
10         if the p-cycle shares link(s) with C+_inter then
11             implement the FS-layer assignment of C+_inter
               on the p-cycle;
12             flag = TRUE;
13             break;
14         end
15     end
16     if flag = FALSE then
17         select one Hamiltonian p-cycle randomly;
18         implement the FS-layer assignment of C+_inter on
           the p-cycle;
19     end
20 end
21 build p-cycle C-_inter in the opposite direction of C+_inter;
22 assign FS' [1, ⌈F/2⌉] on C-_inter as backup FS-layer;
23 assign FS' [⌈F/2⌉ + 1, F] on C-_inter as working FS-layer;
24 replace C+_inter with C-_inter and repeat Lines 8-21;
25 assign all FS' on straddling links as working FS-layer;
```

## V. Performance Evaluation

### A. Simulation Setup and Scenarios

We evaluate the performance of the proposed algorithms for dynamic *p*-cycle protection design in EONs, i.e., PWCE-*p*-cycle-SP, Ham-*p*-cycle-SP and P-Ham-*p*-cycle-SP, using numerical simulations. We assume that the bandwidth of each FS is 12.5 GHz and each fiber link can accommodate $F = 358$ FS'. The dynamic requests are generated according to the Poisson process. For each request, we choose the source and destination pair $s$-$d$ randomly. The number of FS' required by each request, $n$, is uniformly distributed within $[3, 20]$.

The simulations are performed with two topologies, the NSFNET topology in Fig. 2(a) and the US Backbone (USB) topology in Fig. 7. The ILP models use $\mathbb{C}$ that contains 518 shortest cycles for the NSFNET topology, while for the USB topology, $\mathbb{C}$ has 2991 shortest cycles in it. The cycles are calculated with the algorithm developed in [25]. PWCE-*p*-cycle-SP configures three *p*-cycles as *Cycles* 1-3 in Fig. 2(b) for the NSFNET topology with $\gamma = 11$ and assigns FS' $[1, 90]$, $[91, 180]$ or $[181, 270]$ on them as their backup FS-layers, respectively. Then, the same blocks of FS' on the links that are protected by these *p*-cycles, are assigned to the working FS-layer. All the remaining FS' in the network are reserved for the hybrid FS-layer. For instance, since FS' $[1, 90]$ on *Cycle* 1 are assigned to the backup FS-layer and *Cycle* 1 protects *Link* 3→6, FS' $[1, 90]$ on *Link* 3→6 are for the working FS-layer. While the rest of FS' on *Link* 3→6, i.e., $[91, 358]$, are reserved for the hybrid FS-layer. Similarly, for the USB topology, PWCE-*p*-cycle-SP configures five *p*-cycles with $\gamma = 12$ and assigns FS' $[1, 90]$, $[91, 180]$, or $[181, 270]$ to the backup FS-layers on them. For Ham-*p*-cycle-SP and P-Ham-*p*-cycle-SP, we only need to configure the working and backup FS-layers for two *p*-cycles in the whole topology or a domain, and hence the spectrum planning assigns FS' $[1, 179]$ and $[180, 358]$ to the FS-layers. In the simulations, we compare the proposed *p*-cycle protection scheme with the SPP scheme in [18]. The SPP algorithm also targets for 100% restoration against single-link failures. In order to achieve fair comparison between SPP and the *p*-cycle based algorithms, we also implement $K$ shortest-path routing for it. More specifically, for each request, SPP calculates $K$ shortest link-disjoint paths, assigns the shortest one as the working path, and then among the rest paths, selects the shortest one that has sufficient FS' as the backup path. Meanwhile, it tries to encourage sharing of the backup spectrum resources between connections whose working paths are link-disjoint during the spectrum assignment.

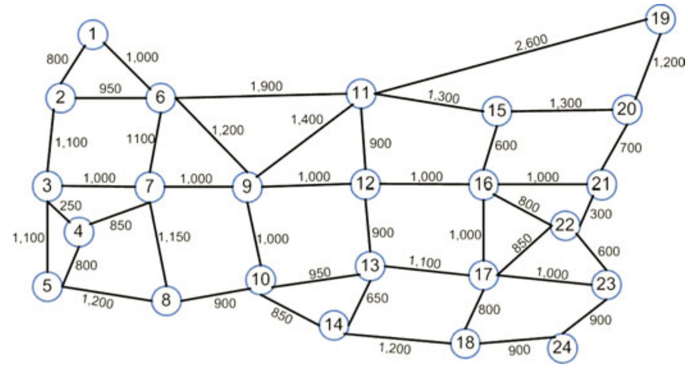

Fig. 7. US Backbone topology (fiber lengths in kilometers).

### B. Blocking Probability

Fig. 8 shows the simulation results on the request blocking probability. For P-Ham-*p*-cycle-SP, we partition the topology into 2 or 3 domains and 4 or 6 domains for the NSFNET and USB topologies, respectively. We can see that in both topologies, PWCE-*p*-cycle-SP provides the highest blocking probability. This is because setting up and tearing down working and backup resources frequently in the hybrid FS-layer lead to significant spectrum fragmentation. Ham-*p*-cycle-SP achieves the lowest blocking probabilities in both topologies due to the efficient protection design and spectrum planning. Note that the results in Fig. 8(a) show that the blocking performance of P-Ham-*p*-cycle-SP with 2 domains is comparable to that of Ham-*p*-cycle-SP. We also observe that the blocking performance of

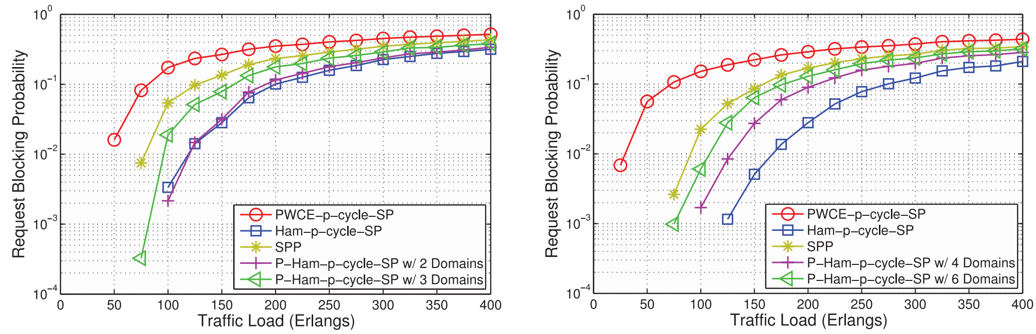


(a) (b)

Fig. 8. Simulation results on request blocking probabilities. (a) NSFNET topology. (b) US Backbone topology.

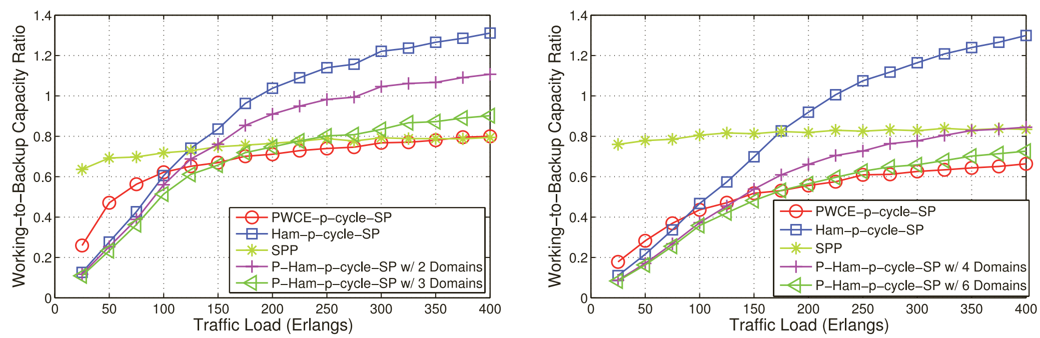


(a) (b)

Fig. 9. Simulation results on working-to-backup capacity ratio. (a) NSFNET topology. (b) US Backbone topology.

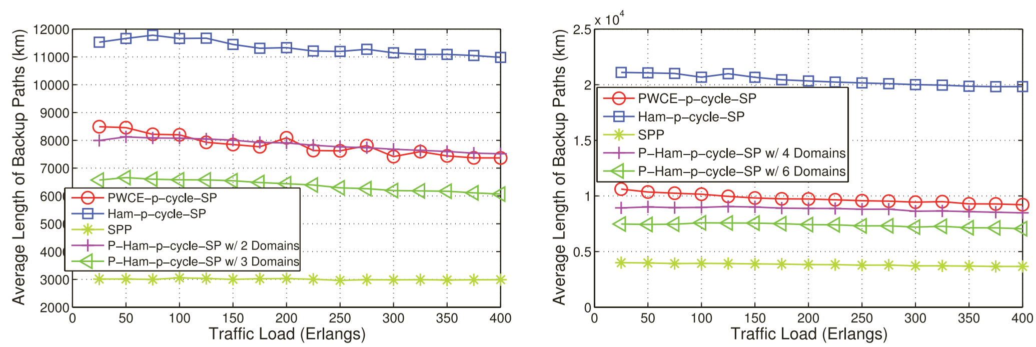


(a) (b)

Fig. 10. Simulation results on average length of backup paths per request. (a) NSFNET topology. (b) US Backbone topology.

P-Ham-*p*-cycle-SP becomes worse when the number of domains increases. This is because when the topology is partitioned into more domains, P-Ham-*p*-cycle-SP has to use more links to protect a working path that traverses multiple domains. Ham-*p*-cycle-SP and P-Ham-*p*-cycle-SP provide better blocking performance than SPP in both topologies, which verifies their effectiveness.

### C. Working-to-Backup Capacity Ratio

Fig. 9 illustrates the simulation results on the working-to-backup capacity ratio (WtB-CR). Here, we define WtB-CR as the ratio of total working FS' to total backup FS'. Fig. 9 shows that in both topologies, when the traffic load increases, the WtB-CR of SPP increases slightly and then stays around 0.8. This is because SPP does not reserve FS' as backup resources, but sets up and tears down both the working and backup paths dynamically. For the proposed *p*-cycle-based algorithms, the FS' in the backup FS-layers are pre-reserved, and therefore their WtB-CRs increase gradually with the traffic load, when more working paths are accommodated in the network. Benefiting from the spectrum planning with the Hamiltonian cycles, Ham-*p*-cycle-SP and P-Ham-*p*-cycle-SP can provide comparable or even larger WtB-CR than SPP for high traffic loads. Since compared with Ham-*p*-cycle-SP and P-Ham-*p*-cycle-SP, PWCE-*p*-cycle-SP reserves smaller number of FS' for the backup FS-layer, PWCE-*p*-cycle-SP provides larger WtB-CRs for low traffic loads. It is also worth noting that the WtB-CRs from

P-Ham-*p*-cycle-SP are smaller than those from Ham-*p*-cycle-SP, because P-Ham-*p*-cycle-SP generally uses more links to protect a working path. Also, when P-Ham-*p*-cycle-SP divides the topology into more domains, WtB-CR becomes smaller because the algorithm has to use more links to protect a working path that traverses multiple domains.

### D. Average Length of Backup Paths

Fig. 10 shows the results on average length of backup paths per request. As expected, Ham-*p*-cycle-SP provides the longest average lengths in both topologies. P-Ham-*p*-cycle-SP can greatly reduce the average lengths of backup paths by decomposing the topology into several domains. The more domains it partitions the topology into, the shorter average length of backup paths it can provide. Therefore, P-Ham-*p*-cycle-SP can overcome the long propagation delay and intolerable physical impairments caused by Ham-*p*-cycle-SP. For the PWCE-*p*-cycle-SP in the NSFNET topology, the average lengths are longer than that of the P-Ham-*p*-cycle-SP with 3 domains. In the USB topology, PWCE-*p*-cycle-SP provides longer average lengths than both the P-Ham-*p*-cycle-SP schemes. SPP achieves the shortest average lengths in both topologies, since the backup paths are always set up with one of the $K$ shortest path candidates.

## VI. Conclusion

In this paper, we investigated dynamic *p*-cycle protection design for EONs and proposed several algorithms. By combining PWCE-*p*-cycle design with spectrum planning, we first designed an algorithm that could achieve dynamic *p*-cycle design in EONs. Then, in order to resolve the coverage issue of the PWCE-*p*-cycles, we considered dynamic *p*-cycle design with Hamiltonian cycles and proposed to use topology partition for reducing the lengths of backup paths. The simulation results showed that our proposed algorithms could achieve lower blocking probability than the SPP algorithm, while the average length of backup paths per request could be controlled well.

## References

[1] J. Armstrong, "OFDM for optical communications," *J. Lightw. Technol.*, vol. 27, no. 3, pp. 189–204, Mar. 2009.

[2] O. Gerstel, M. Jinno, A. Lord, and B. Yoo, "Elastic optical networking: A new dawn for the optical layer?," *IEEE Commun. Mag.*, vol. 50, no. 2, pp. S12–S20, Apr. 2012.

[3] M. Jinno *et al.*, "Distance-adaptive spectrum resource allocation in spectrum-sliced elastic optical path network," *IEEE Commun. Mag.*, vol. 48, no. 8, pp. 138–145, Aug. 2010.

[4] Y. Wang, X. Cao, and Y. Pan, "A study of the routing and spectrum allocation in spectrum-sliced elastic optical path networks," in *Proc. IEEE Int. Conf. Comput. Commun.*, Apr. 2011, pp. 1503–1511.

[5] K. Christodoulopoulos, I. Tomkos, and E. Varvarigos, "Elastic bandwidth allocation in flexible OFDM-based optical networks," *J. Lightw. Technol.*, vol. 29, no. 9, pp. 1354–1366, May 2011.

[6] Z. Zhu, W. Lu, L. Zhang, and N. Ansari, "Dynamic service provisioning in elastic optical networks with hybrid single-/multi-path routing," *J. Lightw. Technol.*, vol. 31, no. 1, pp. 15–22, Jan. 2013.

[7] M. Klinkowski and K. Walkowiak, "Routing and spectrum assignment in spectrum sliced elastic optical path network," *IEEE Commun. Lett.*, vol. 15, no. 8, pp. 884–886, Aug. 2011.

[8] Y. Sone *et al.*, "Routing and spectrum assignment algorithm maximizes spectrum utilization in optical networks," in *Proc. Eur. Conf. and Exhibition Optical Communication*, Sep. 2011, pp. 1–3.

[9] L. Gong, X. Zhou, W. Lu, and Z. Zhu, "A two-population based evolutionary approach for optimizing routing, modulation and spectrum assignments (RMSA) in O-OFDM networks," *IEEE Commun. Lett.*, vol. 16, no. 9, pp. 1520–1523, Sep. 2012.

[10] S. Ramamurthy, L. Sahasrabuddhe, and B. Mukherjee, "Survivable WDM mesh networks," *J. Lightw. Technol.*, vol. 21, no. 4, pp. 870–883, Apr. 2003.

[11] J. Cai *et al.*, "20 Tbit/s transmission over 6860 km with Sub-Nyquist channel spacing," *J. Lightw. Technol.*, vol. 30, no. 4, pp. 651–657, Feb. 2012.

[12] Y. Sone *et al.*, "Bandwidth squeezed restoration in spectrum-sliced elastic optical path networks (SLICE)," *J. Opt. Commun. Netw.*, vol. 3, pp. 223–233, Mar. 2012.

[13] S. Xu *et al.*, "Shared-path protection in OFDM-based optical networks with elastic bandwidth allocation," in *Proc. Opt. Fiber Commun. Conf. Expo.*, Mar. 2012, pp. 1–3.

[14] A. Castro, L. Velasco, M. Ruiz, and J. Comellas, "Single-path provisioning with multi-path recovery in flexgrid optical networks," in *Proc. Int. Congr. Ultra Modern Telecommun. Control Syst. Workshops*, Oct. 2012, pp. 745–751.

[15] M. Klinkowski and K. Walkowiak, "Offline RSA algorithms for elastic optical networks with dedicated path protection consideration," in *Proc. Int. Congr. Ultra Modern Telecommun. Control Systems and Workshops*, Oct. 2012, pp. 670–676.

[16] A. Eira, J. Pedro, and J. Pires, "Spectrum and transponder optimization in survivable translucent flexible-grid optical networks," in *Proc. Int. Conf. Commun.*, Jun. 2012, pp. 6235–6240.

[17] X. Cai *et al.*, "Experimental demonstration of adaptive combinational QoT degradation restoration in elastic optical networks," *J. Lightw. Technol.*, vol. 31, no. 4, pp. 664–671, Feb. 2013.

[18] M. Liu, M. Tornatore, and B. Mukherjee, "Survivable traffic grooming in elastic optical networks—shared protection," *J. Lightw. Technol.*, vol. 31, no. 6, pp. 903–909, Mar. 2013.

[19] W. Shi, Z. Zhu, M. Zhang, and N. Ansari, "On the effect of bandwidth fragmentation on blocking probability in elastic optical networks," *IEEE Trans. Commun.*, vol. 61, no. 7, pp. 2970–2978, Jul. 2013.

[20] W. Grover and D. Stamatelakis, "Cycle-oriented distributed preconfiguration: Ring-like speed with mesh-like capacity for self-planning network restoration," in *Proc. Int. Conf. Commun.*, Jun. 1988, pp. 537–543.

[21] D. Schupke, C. Gruber, and A. Autenrieth, "Optimal configuration of p-cycles in WDM networks," in *Proc. Int. Conf. Commun.*, Jun. 2002, pp. 2761–2765.

[22] H. Huang and J. Copeland, "A series of Hamiltonian cycle-based solutions to provide simple and scalable mesh optical network resilience," *IEEE Commun. Mag.*, vol. 40, no. 11, pp. 46–51, Nov. 2002.

[23] Z. Zhang, W. Zhong, and B. Mukherjee, "A heuristic method for design of survivable WDM networks with p-cycles," *IEEE Commun. Lett.*, vol. 8, no. 7, pp. 467–469, Jul. 2004.

[24] Z. Zhang, W. Zhong, and S. Bose, "Dynamically survivable WDM network design with p-cycle-based PWCE," *IEEE Commun. Lett.*, vol. 9, no. 8, pp. 756–758, Aug. 2005.

[25] A. Eshoul and H. Mouftah, "Survivability approaches using p-cycles in WDM mesh networks under static traffic," *IEEE/ACM Trans. Netw.*, vol. 17, no. 2, pp. 671–683, Apr. 2009.

[26] W. Grover, "The protected working capacity envelope concept: An alternate paradigm for automated service provisioning," *IEEE Commun. Mag.*, vol. 42, no. 1, pp. 62–69, Jan. 2004.

[27] W. Zhong and Z. Zhang, "Design of survivable WDM networks with shared-p-cycles," in *Proc. Opt. Fiber Commun. Conf. Expo.*, Mar. 2004, pp. 554–556.

[28] L. Long and A. Kamal, "p2-cycles: p-cycles with parasitic protection links," in *Proc. Int. Conf. Commun.*, Jun. 2010, pp. 1–5.

Authors' biographies not available at the time of publication.